NASA TECHNICAL
MEMORANDUM

NASA TM X-52431

A RESUME OF RESEARCH ON COAXIAL PLASMA
GUNS PERFORMED AT LEWIS RESEARCH CENTER

by Charles J. Michels
Lewis Research Center
Cleveland, Ohio

NATIONAL AERONAUTICS AND SPACE ADMINISTRATION · WASHINGTON, D.C. · 1968

A RESUME OF RESEARCH ON COAXIAL PLASMA GUNS

PERFORMED AT LEWIS RESEARCH CENTER

by Charles J. Michels

Lewis Research Center
Cleveland, Ohio

TECHNICAL PAPER presented at

NATIONAL AERONAUTICS AND SPACE ADMINISTRATION

A RESUME OF RESEARCH ON COAXIAL PLASMA GUNS

PERFORMED AT LEWIS RESEARCH CENTER*

by Charles J. Michels

Lewis Research Center
National Aeronautics and Space Administration
Cleveland, Ohio

SUMMARY

This resume of research on coaxial plasma guns at the Lewis Research Center
describes an effort to determine the potential of the gun for space propulsion applications.
The experimental parametric examination of various gun geometries, the theoretical
analysis of capacitor-bank - variable-mass distribution gun systems, and the plasma
diagnostics of various geometries is summarized. The results of this program indicated
that the efficiency (≈40 percent) was too low to be competitive with alternative systems.
Propellant, switching, and heat-rejection systems proved to be complicated.

INTRODUCTION

From 1962 to 1967, a series of experiments with coaxial plasma guns (all powered
by conventional capacitor banks) was conducted at Lewis. These experiments were per-
formed to determine the possible application of the gun to electrical space propulsion.
Thus the direction of the research emphasized performance and understanding of the
physics of the acceleration of plasma in the gun. The research at Lewis Research Center
has been reported in references 1 to 7, and a survey of other NASA-sponsored research
on propulsion-oriented guns is described in reference 8. At first the experiments were
performed to examine performance for various parametric cases (refs. 1 and 2). Then
an analytical model was proposed and compared with the experiments (refs. 2 to 4). The
analysis was given for various nondimensional parameters. The values of these param-

---

E-4428

eters for optimizing gun performance were described. An experimental evaluation of the system characteristics of the capacitor bank powering these experiments is given in reference 7. Other physics aspects of the accelerator which were investigated were self-crowbarring discharge diagnosis (ref. 1), time-integrated spectra of the plasma in guns (ref. 3), transient electrical and optical characteristics of the gun exhaust (refs. 4 and 6), transient spectra of the plasma in guns (refs. 4 and 5), magnetic probing of the gun annulus (refs. 1, 3, and 4), and improved methods for gun voltage and current recording (ref. 4). A brief discussion of each of these endeavors is presented herein.

PERFORMANCE OF GUN - CAPACITOR-BANK SYSTEMS

The results of the initial investigation on gas-puff-operated, single-shot, coaxial guns were reported by Michels and Ramins (ref. 1). An illustration of the gun is shown in figure 1. The effects of various propellants on gun performance were examined, and the results are shown in figures 2 and 3. Argon performed best, but the kinetic efficiencies were low. An operating map of the gun, operating self-crowbarred, was provided by this research.

The numerous gun geometries and various energy storage systems used to power these guns that were discussed at the International Symposium on Coaxial Plasma Guns (Case Institute of Technology, September, 1962) served to stimulate Lewis interest in providing an analytical model that fit most of these systems. The model would help in directing propulsion-oriented gun research for higher efficiency geometries and systems. The results of this analytical effort along with new experimental data for three different gun geometries were presented by Michels, Heighway, and Johansen in reference 2. The gun circuit used for this analysis is shown in figure 4. Three coupled, nonlinear equations describing the circuit, the plasma momentum (assuming a snowplow model), and the plasma energy were set down. In order to generalize the equations and to facilitate their solution, nondimensional variables and parameters were introduced.

For a given gun geometry, only two of these parameters are easily varied experimentally: the mass loading parameter $\mathcal{M}$ and the mass distribution parameter α. The parameter $\mathcal{M}$ is defined as

$$\mathcal{M} = \left(\frac{2l}{L'C^2V_o^2}\right)M_o \tag{1}$$

In the theory of reference 1, the mass distribution in the x-direction $M_o(df/dx)$ was so chosen that a family of distributions could be presented from a slug to a constant-density profile. The function

$$f = 1 - (1 - \xi)^{1/(1-\alpha)} \qquad (2)$$

was used, in which α can be varied from 0 (constant density) to 1 (slug). In all the references cited herein $\alpha = 0.5$ was chosen to approximate the experimental distribution. The symbols used are

ξ nondimensional length, $\ell^{-1}x$

M_O total mass swept up per shot, kg

x   distance of current sheet from initial discharge location, m

t   time, sec

C   capacitance of bank, F

V_O initial capacitor voltage, V

ℓ effective gun length, m

L'   gun inductance per unit length, H/m

The theoretical kinetic efficiency is defined as

$$\eta_2 \equiv \frac{\frac{1}{2} M_O \left(\frac{dx}{dt}\right)^2}{\frac{1}{2} C V_O^2} \quad x = \ell \qquad (3)$$

A nondimensional exit velocity $\dot{\xi}$ is defined in reference 3 as

$$\dot{\xi} \equiv \sqrt{\frac{L'C}{\ell}} \left(\frac{dx}{dt}\right)_{x=\ell} \qquad (4)$$

The three coupled equations were solved for various values of the parameters, and the results are discussed in reference 2. Then experimental results were compared with the predicted performance. The optimum value of the mass loading parameter $\mathcal{M}$ is near 1. The optimum value of the nondimensional inductance $\mathcal{L}$ where

$$\mathcal{L} = \frac{L}{L'\ell} \qquad (5)$$

is near 0.1. Here, L is the system initial inductance in henries. As shown in figure 5, the theoretical kinetic efficiency for these optimum values increases monotonically from 27 to 93 percent as the mass distribution is varied from uniform to the slug distribution.

The optimum exit velocity is also shown in figure 5. The figure provides the design criteria for optimum performance of simple capacitor-driven, cylindrically symmetrical, coaxial plasma guns with variable mass distribution. Experimentally stable operation of the gun has been limited to cases for which a simplified analysis limits theoretical efficiency to about 40 percent. In reference 2, experimentally measured efficiencies are approximately half those predicted with the simplified analysis. In later work (refs. 3 and 4), experimentally measured efficiencies are much closer to the values predicted with the simplified analysis (see fig. 6(b)). The simplified analysis is a special case of a more complete theory presented in reference 2 and extended in reference 3. The more complete theory takes into account various plasma losses and predicts more closely the experimentally observed performances. A typical comparison of data (experimental and theoretical) for a particular gun geometry is shown in figure 6(b). The analysis agrees rather well with the experiment for this case, yet for some geometries (e.g., fig. 6(a) agreement was poor. Time-integrated-spectra results pointed to the need for determining when the contaminants would affect the results. Other system losses were accounted for in an analysis based on the examination (performed earlier, in 1965) of the capacitor bank (see fig. 7). The examination consisted of studying the electrical characteristics of the bank and making a transient energy inventory of its ignitron switches. This study is reported in reference 7.

DISCHARGE CHARACTERISTICS

During the 5-year period of research on plasma guns, various experiments were performed aimed at understanding the nature of the plasma and the acceleration phenomena. The knowledge obtained from those experiments is needed to determine thrust and the effects of the exhaust plasma on exhaust instrumentation (calorimeters and various probes). In this work, argon was used as the propellant. Reference 6 describes the results of an experimental investigation of the discharge from a self-crowbarred gun, using Rogovsky loops, framing and streak cameras, and magnetic field probes. Frame views of the exhaust from that gun are shown in figure 8. From these measurements, an exhaust model was proposed (shown in fig. 9). The exhaust has the following three separate characteristics:

(1) There are relatively few fast particles out in front and no significant currents flow in this plasma.

(2) These particles are followed by a diffuse plasma (not carrying axial currents) predicted in position and velocity as if it were an extrapolation of the magnetic front noted in the gun annulus.

(3) This plasma is followed by a later developing cylindrically symmetric pinch-core

structure (carrying gross axial currents still connected to the electrodes). By the time this pinch-core had moved downstream to impinge on a calorimeter, the currents were insignificant. The experiment demonstrated the velocity spectrum and time sequence of various phases of the exhaust from the device.

The influence of contaminants on performance was examined during a series of experiments (refs. 4 and 5) performed on two different gun geometries. One geometry exhibited relatively good performance; the other showed poorer than predicted performance and not reproducible operation. Preliminary results were presented by Michels and Hettel in reference 5. A portion of the typical transient spectrum for a self-crowbarred gun is shown in figure 10, along with the corresponding time-integrated spectrum. For this gun, performance agrees with theory and the time-varying spectrum exhibits a fully ionized argon propellant plasma (relatively "clean") for the first moving discharge in the gun. In contrast, the other geometry which operated in the multiple-moving-puff mode exhibits a contaminated discharge with no propellant lines observed. A pyrex baffle is the source of contaminants. Performance did not agree with theory.

In reference 4, the many stationary and moving discharges (in guns with two different modes of operation) are delineated through magnetic probes, frame and streak views of the discharge, and the transient spectra. The distance-time diagram of discharges in the self-crowbarred gun is shown in figure 11. A transient spectrometer, employing a grating polychromer whose spectral output was recorded by an image converter camera (used in streak mode), and a transient voltage digitizer used in gathering performance data are also described in reference 4.

CONCLUDING REMARKS

Research on single-shot coaxial plasma guns was undertaken at the NASA Lewis Research Center to determine the potentiality of the gun for space propulsion applications. This research was part of a NASA-sponsored program of study of coaxial guns in federal, industrial, and university laboratories.

The results of this program indicated that the efficiency ($\approx$40 percent) was too low to be competitive with alternative systems. The potentiality of the gun might increase significantly if the spoke instabilities that occur for slug mass distributions could be suppressed and if the programmed payout of energy from the energy source could be coupled optimumly to a tailored gun geometry. Although not seriously examined in this program,

propellant systems, energy switching systems, and heat-rejection problems of the electrodes appear to be complicated.

REFERENCES

1. Michels, Charles J.; and Ramins, Peter: Performance of Coaxial Plasma Gun with Various Propellants. Phys. Fluids, vol. 7, no. 11, pt. 2, Nov. 1964, pp. S71-S74.

2. Michels, C.J.; Heighway, J.E.; and Johansen, A.E.: Analytical and Experimental Performance of Capacitor Powered Coaxial Plasma Guns. AIAA J., vol. 4, no. 5, May 1966, pp. 823-830.

3. Michels, Charles J.; and Johansen, Albert E.: Experimental and Theoretical Performance of Coaxial Plasma Guns. NASA TN D-3469, 1966.

4. Michels, Charles J.; and Hettel, Henry J.: Correlation of Transient Spectra with Performance in Coaxial Plasma Guns. NASA TN D-4385, 1968.

5. Michels, Charles J.; and Hettel, Henry J.: Transient Spectral Study of Discharges in Coaxial Plasma Guns. Proceedings of the American Physical Society Topical Conference on Pulsed High-Density Plasmas. Rep. LA-3770, Los Alamos Scientific Lab., Sept. 29, 1967, pp. E6-1 to E6-5.

6. Michels, Charles J.: Some Transient Electrical Characteristics of the Exhaust of a Self-Crowbarred Coaxial Plasma Gun. NASA TN D-2571, 1965.

7. Michels, Charles J.; and Terdan, Fred F.: Characteristics of a 5-Kilojoule, Ignitron-Switched, Fast-Capacitor Bank. NASA TN D-2808, 1965.

8. Domitz, Stanley; Kosmahl, H.G.; Ramins, Peter; and Stevens, N. John: Survey of Electromagnetic Accelerators for Space Propulsion. NASA TN D-3332, 1966.
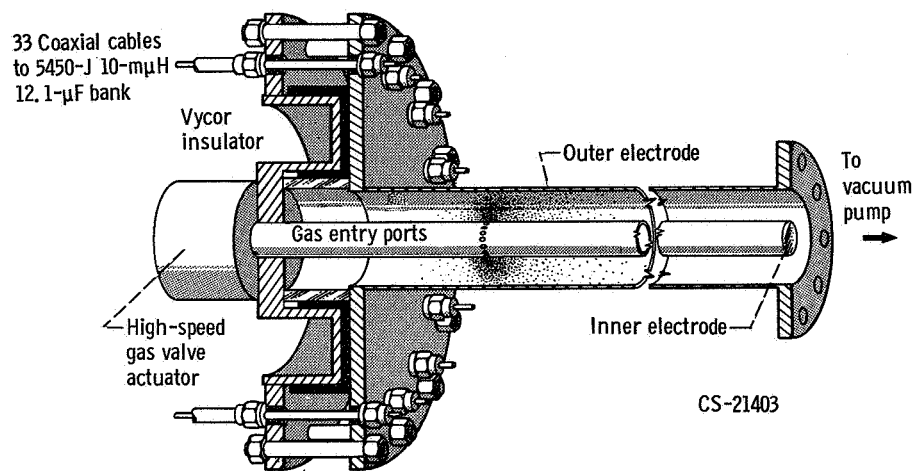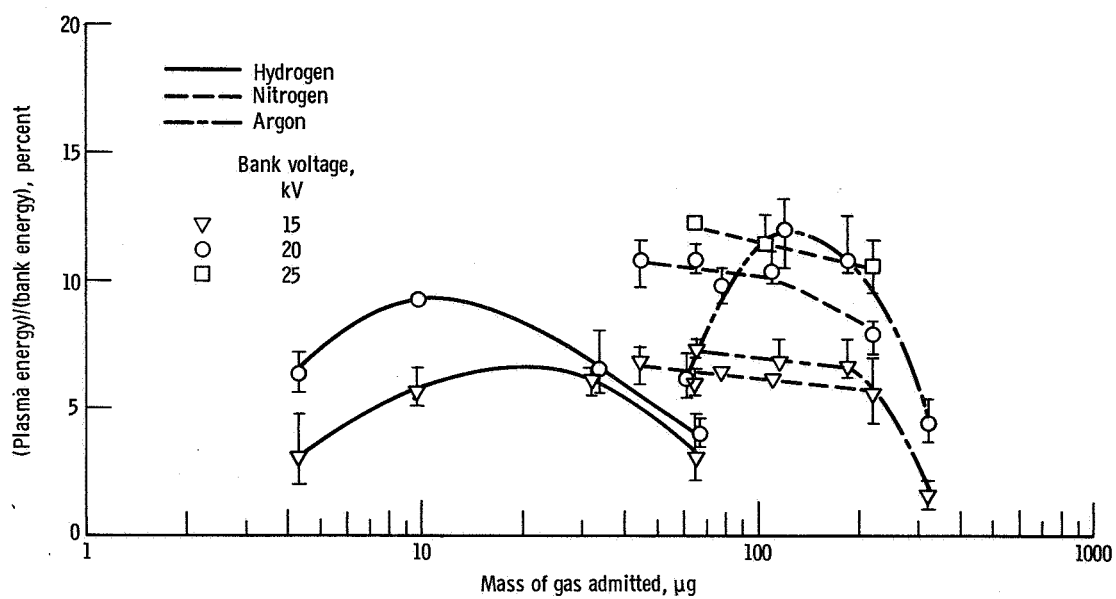
Figure 1. - Coaxial plasma gun.

Figure 2. - Effect of mass of propellant admitted on system efficiency for different bank voltages.
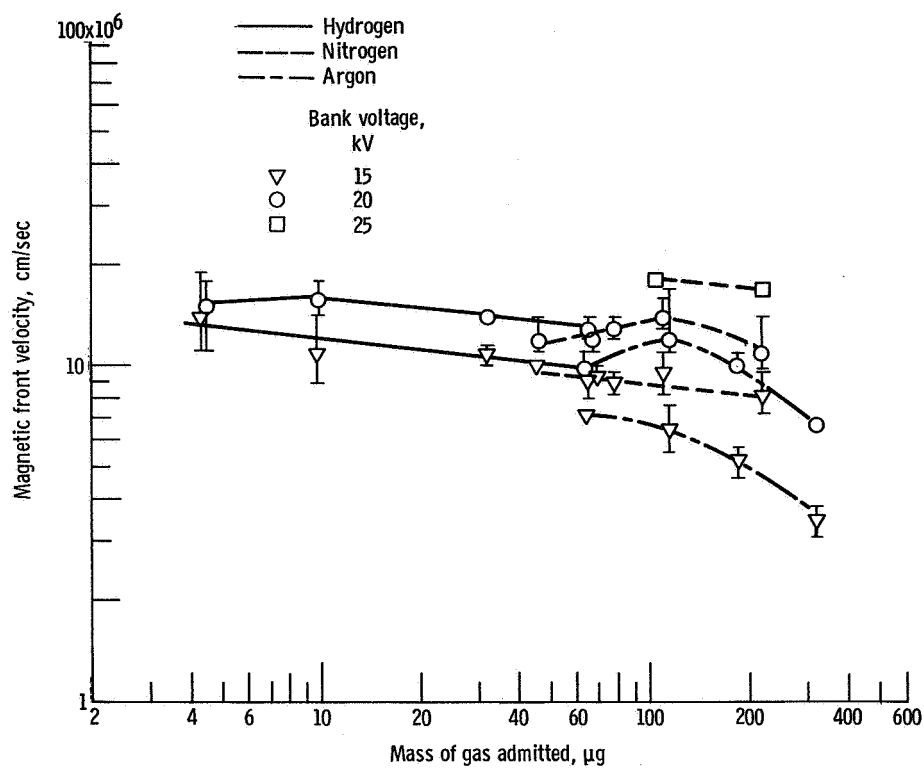
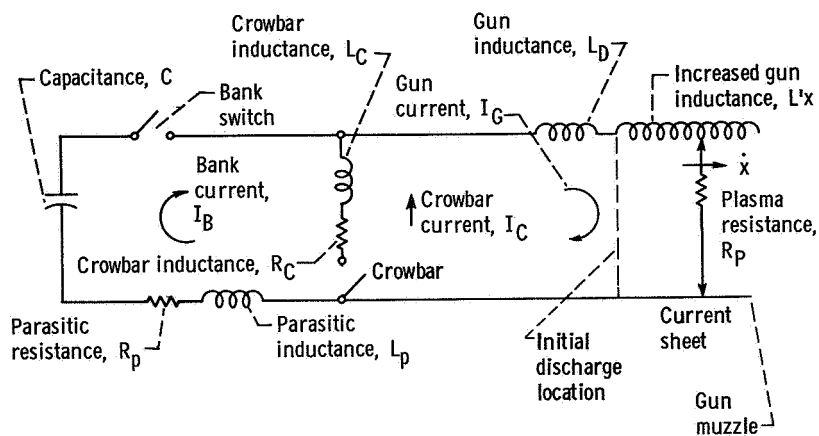Figure 3. - Effect of admitted mass and bank voltage on magnetic front velocity.
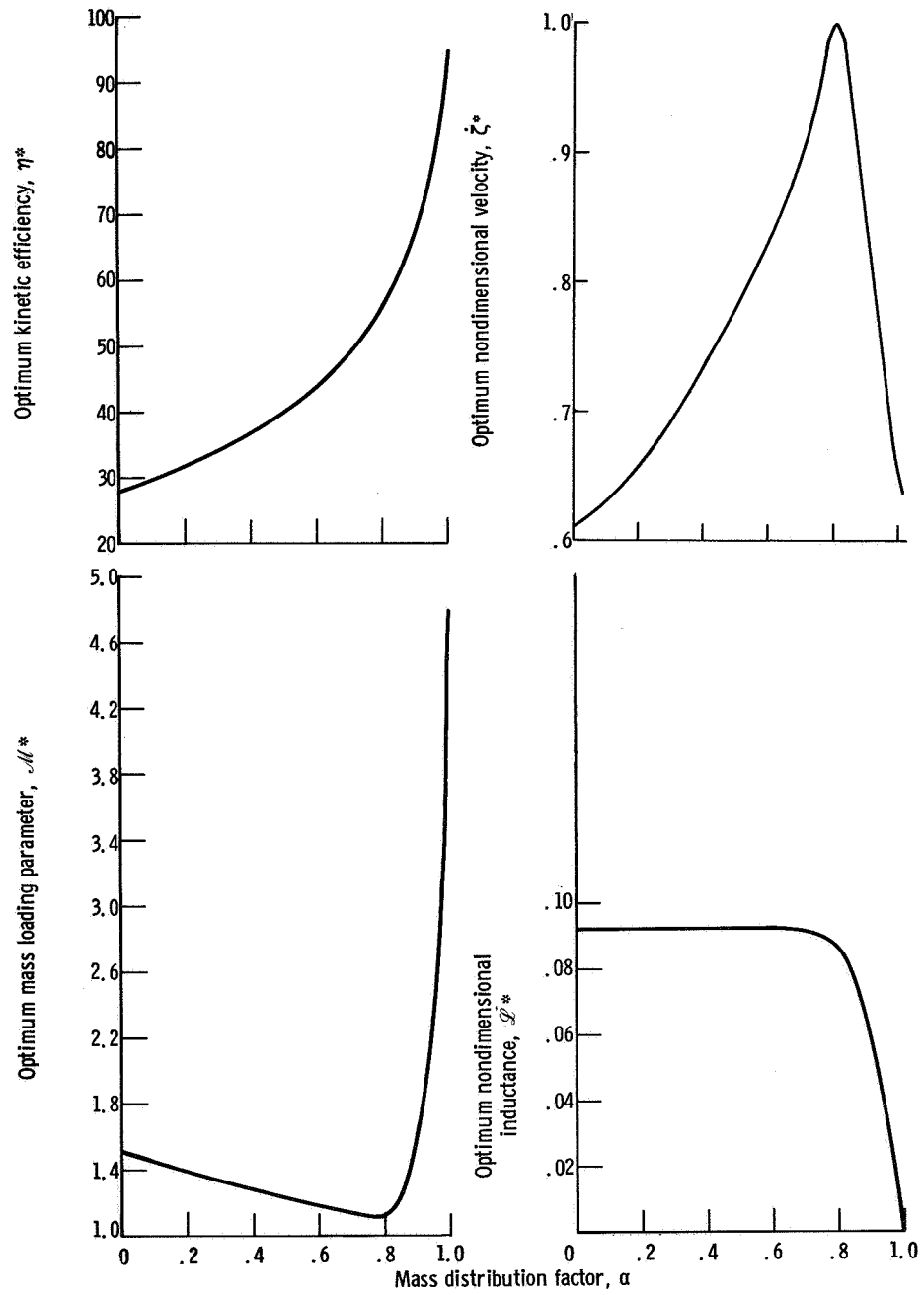

Figure 4. - Equivalent gun circuit.

Figure 5. – Theoretical optimum kinetic efficiency for simplified model.

Model
— — — Simplified
— — — Loss

Initial bank
voltage,
kV
◇ ⟁ 15
▢ 18
□ 19
◌ ◐ 20
◍ 22
◁ ◀ 25

Solid symbols denote present
data
Open symbols denote data
of ref. 3

Efficiency, η, percent

Velocity, ξ, nondimensional

Velocity, $\frac{dx}{dt}$, cm/μsec

Mass loading parameter, $\mathscr{M}$
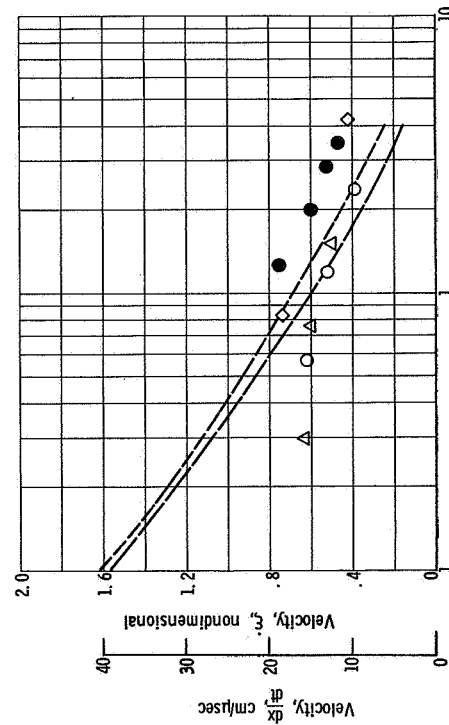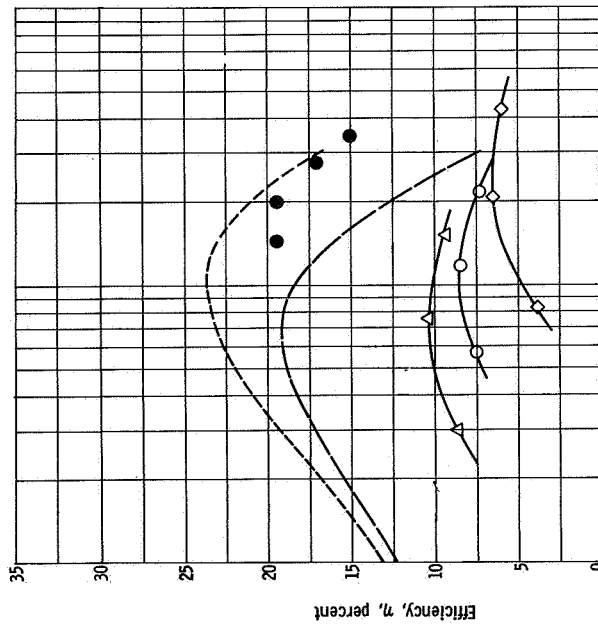
(a) Noncrowbarred geometry.
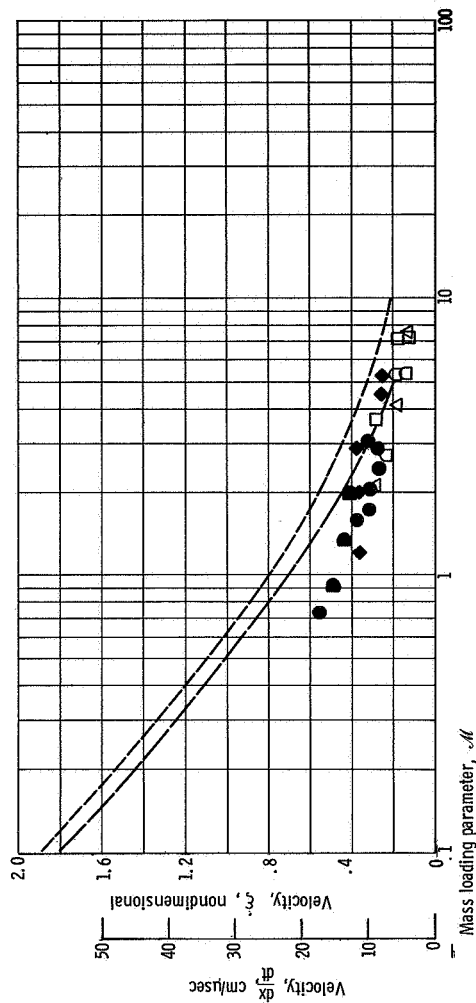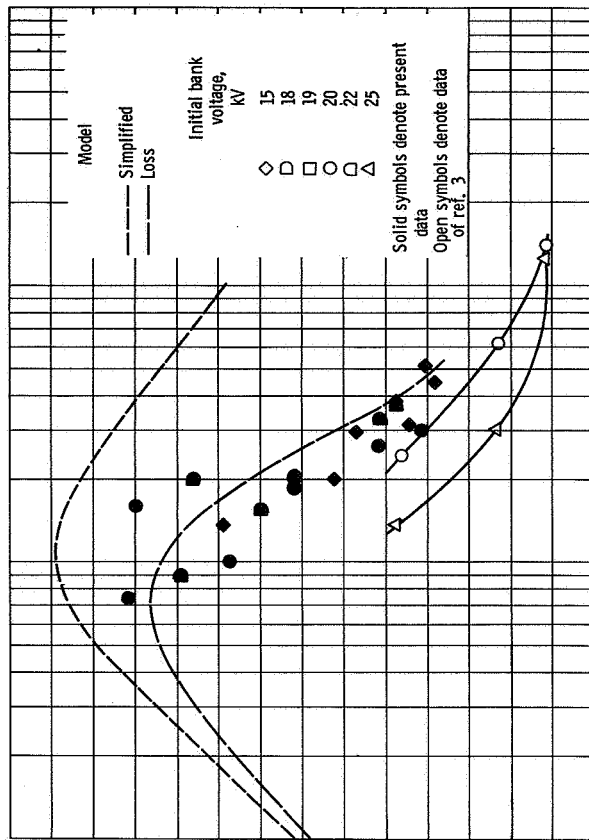
(b) Self-crowbarred geometry. Theoretical model crowbarred at maximum energy.

Figure 6. – Theoretical and experimental performance of plasma-gun geometries. Mass distribution parameter, 0.5.

Figure 7. - Capacitor bank.

Magnetic probe

Coaxial plasma gun

Glass cross

Rogovsky loop (R$_S$)

Event	Time, μsec	Rogovsky loop view	Muzzle view
Diffuse plasma leaves gun	$T_0 + 3.7$		
	$T_0 + 3.9$		
Plasma core develops connected to gun center electrode	$T_0 + 4.5$		
	$T_0 + 5.0$		
Plasma core threads Rogovsky loop	$T_0 + 5.3$		
	$T_0 + 5.5$		

C-72107

Rogovsky loop probe (illuminated by impingement light)

Stored mirror face

Core of plasma

Camera graticule lines

Rear support plate (reflected light)

Figure 8. – Frame views of gun exhaust.
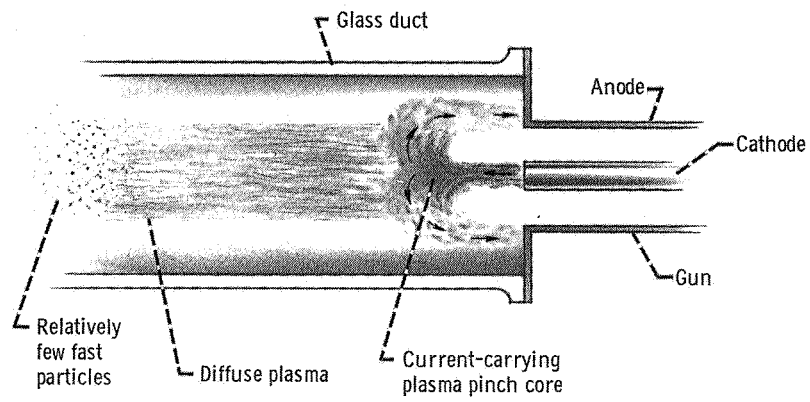
Figure 9. - Exhaust model.   CD-7900

Discharge	Wavelength, Å	Species
Ar III 3729.29		2
O II 3749.47		3
Si III 3791.13		2 to 3
Si III 3796.18		2 to 3
Si III 3806.60		2 to 3
Ar II 3850.57		2
Si II 3853.66		4 to 6
Si II 3856.09		4 to 6
Si II 3862.51		4 to 6
Ar II 3868.53		2
Si III 3924.44		2 to 3
Ar II 3928.62		2
Ar II 3968.36		2
Ar II 4013.87		2
Ar II 4042.91		2
O II 4069.90		3 to 5
Ar II 4072.01		3 to 5
O II 4072.16		3 to 5
O II 4075.87		3 to 5
Si IV 4088.86		3

Event

Second discharge

Third discharge

Subsequent discharges

Streak stop

$T_0 + 2.6$ $T_0 + 3.6$ $T_0 + 4.6$ $T_0 + 5.6$ $T_0 + 6.6$ $T_0 + 7.6$ $T_0 + 8.6$ $T_0 + 9.6$ $T_0 + 10.6$

Time, μsec

Figure 10. - Self-crowbarred gun spectra. Central wavelength, 3900 Å.

E-4428

Magnetic probes
Outer electrode
Inner electrode

Camera graticule lines

Magnetic probes

4
3
2
1

Masked midbarrel window
with 1.27-cm-long slit

000

Distance, cm
0   10   20   30   40

Time, μsec
0.4 0.6 0.8 1.3 1.8 2.3 50

C-67-4225

Frame views

First discharge
Second discharge
Streak view
Third discharge
Weak subsequent discharges
Crowbar discharge
Gun-current trace
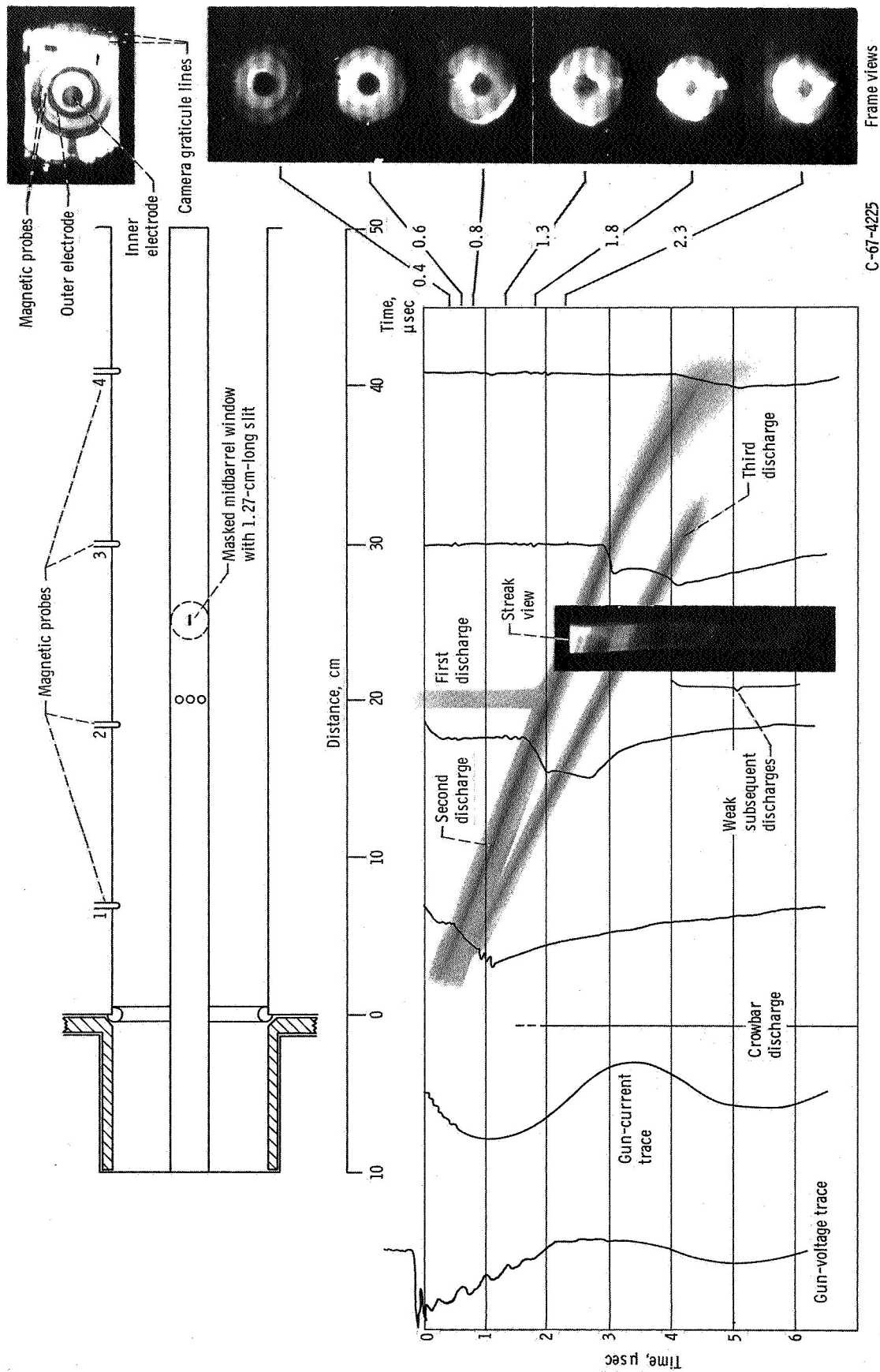Gun-voltage trace

Time, μsec
0   1   2   3   4   5   6

Figure 11. – Distance-time diagram of discharges in self-crowbarred gun.